

Diagnosis of aseptic deep venous thrombosis of the upper extremity in a cancer patient using fluorine-18 fluorodeoxyglucose positron emission tomography/computerized tomography (FDG PET/CT)

B. DO,* C. MARI,**,***,**** S. BISWAL,* J. KALINYAK,* A. QUON* and S.S. GAMBHIR*

**Stanford University Medical Center, Nuclear Medicine Division,
Department of Radiology and Molecular Imaging Program at Stanford (MIPS)*

***San Francisco Veteran Affairs, Nuclear Medicine Division, Department of Radiology*

****UCSF, Nuclear Medicine Program, Department of Radiology and
Center for Molecular and Functional Imaging (CMFI) at China Basin*

We describe a patient with a history of recurrent squamous cell carcinoma of the tongue and abnormal FDG uptake in the left arm during a re-staging FDG PET/CT. After revision of the patient's clinical history, tests and physical exam, the abnormal FDG uptake was found to correspond to an extensive aseptic deep venous thrombosis of the upper extremity.

Key words: FDG PET/CT, aseptic thrombosis, deep venous thrombosis

INTRODUCTION

WE DESCRIBE a patient with a history of recurrent squamous cell carcinoma of the tongue who presented to the clinic for a re-staging FDG PET/CT to evaluate an enlarging left submandibular mass. On the day of evaluation, the patient complained of progressive swelling and constant pain of several days' duration along the medial aspect of the left arm from the axilla to the distal fifth digit. The PET/CT study revealed a peculiar asymmetric, moderately intense, linear FDG uptake distribution in the left upper thoracic region with extension towards the medial aspect of the left arm and forearm. To our knowledge this is the first reported case of increased FDG activity secondary to an extensive aseptic deep venous thrombosis of the upper extremity.

CLINICAL HISTORY

The patient is a 47-year-old male with a history of recur-

rent T4 N0 M0 squamous cell carcinoma of the tongue who had undergone a total glossectomy, laryngectomy, hypopharyngectomy and bilateral neck dissection with free reconstruction and was treated post-operatively with adjuvant combined chemoradiation and external beam radiation to the left neck and anterior thorax. The patient developed an ulcer in the left submandibular region which turned out to be at the surface of a submandibular mass on palpation. The patient was placed on empiric Clindamicin. The mass was biopsy-confirmed to be recurrent squamous cell carcinoma, and a FDG PET/CT scan was requested for re-staging purposes. Five days prior to the scan the patient was hospitalized at Stanford Hospital and Clinics for evaluation of a newly-developed left upper extremity discomfort with non-pitting edema, erythema, and weakness superimposed on his chronic paresthesias in the left neck and shoulder area known to be secondary to the external beam radiation.

At the time of admission, the patient was in no apparent distress. He denied trauma, fever, sweats and chills. His physical exam revealed a pulse of 79 beats per minute (bpm), blood pressure of 140/85, temperature of 36.3, respiratory rate of 20, and saturation of 98% on room air. His left arm was swollen. On his neurological exam he was alert and oriented, with 2+ deep tendon reflexes bilaterally, decreased 4–/5 strength of the left upper extremity on abduction, and 4+/5 strength on adduction.

Received June 3, 2005, revision accepted September 1, 2005.

For reprint contact: Carina Mari Aparici, M.D., University of California, San Francisco (UCSF), Nuclear Medicine, Radiology Department, 505 Parnassus Av, L308E, San Francisco, CA 94143-0252, USA.

E-mail: carina.mari@radiology.ucsf.edu

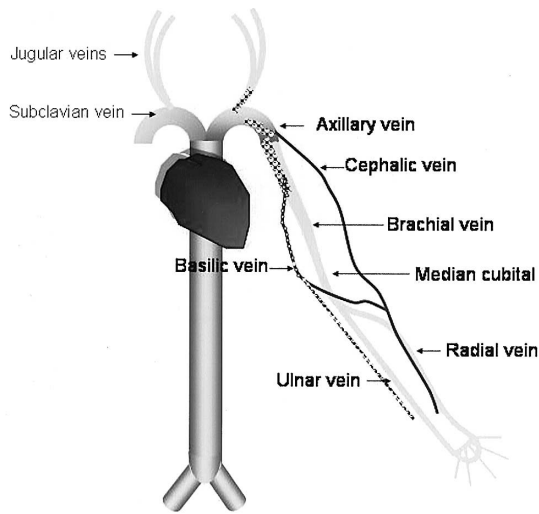


Fig. 1 Diagram of thoracic and upper extremity venous system. The area corresponding to the extensive DVT is shown in a dotted pattern.

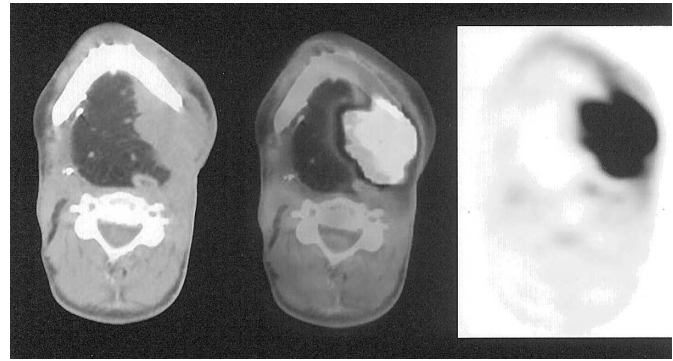


Fig. 2 PET/CT showing intense FDG activity in the left submandibular 5 × 3 cm biopsy-proven recurrent squamous cell carcinoma soft tissue mass (SUVmax of 22). Note the important distortion of the normal neck anatomy after radical surgical resection.

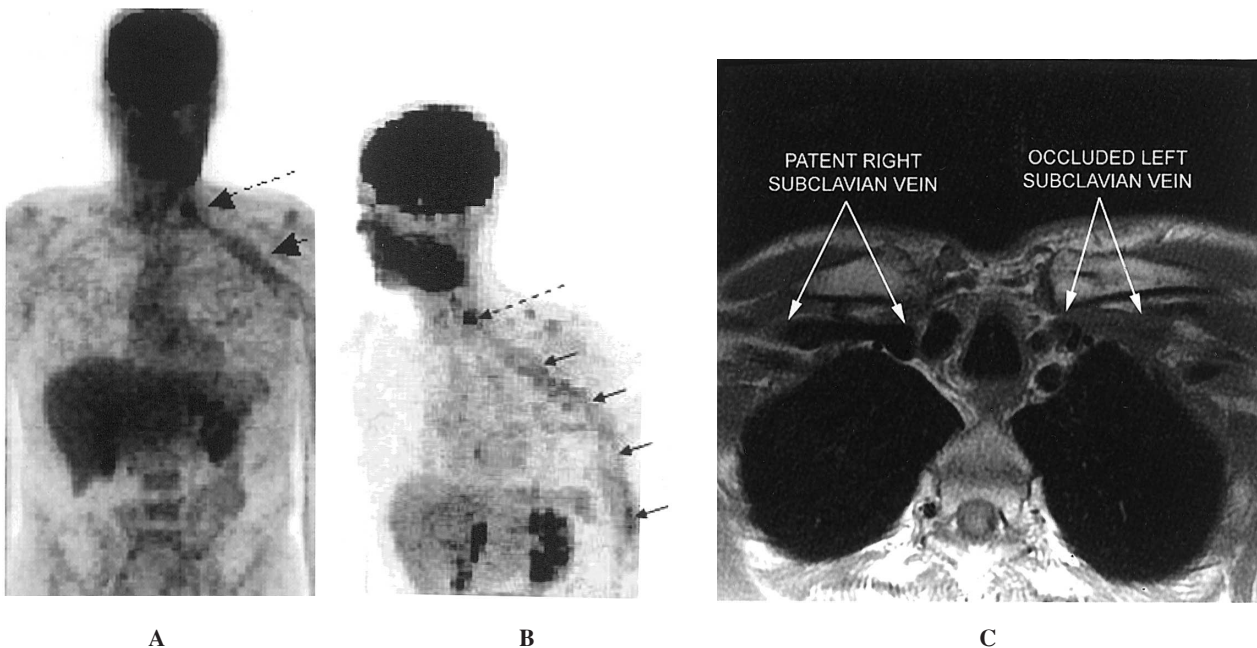


Fig. 3 PET anterior (A) and LAO (B) views showing the trajectory of the aseptic venous thrombosis from left internal jugular vein, left subclavian, axillary vein and basilica vein with reactive left axillary lymphadenopathy in the. Note intense FDG activity in brain and bilateral upper renal collective systems. (C) Transverse T1-weighted MRI image through the subclavian vessels. The normal, patent right subclavian vein shows the normal, dark, low signal flow void expected for patent vessels using this MR technique. In contrast, the abnormal left subclavian vein is filled with intermediate signal (grey) intensity material that is consistent with clot.

His muscle strength in the right upper extremity was 5+/5. His laboratory data on admission included a white cell count of 6.2, hematocrit of 41, platelet count of 524, and INR of 2.0. Urine culture was negative; blood culture obtained from the right hand was negative throughout the admission (5 days).

A venous duplex ultrasound revealed an extensive deep venous thrombosis (DVT) in the left upper extremity extending from the left subclavian vein to the level of the left brachial veins with involvement of the left basilic vein and a non-occlusive clot in the left internal jugular vein (Fig. 1). An MRI and dedicated CT with contrast of the

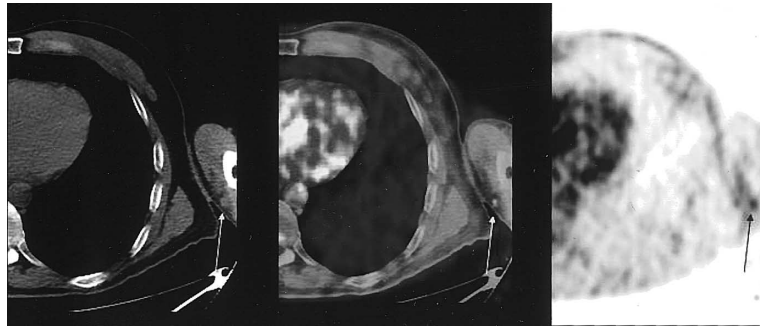


Fig. 4 Moderate FDG activity in the left basilic vein on PET-CT (SUVmax 2.95). Note also moderate activity in myocardium.

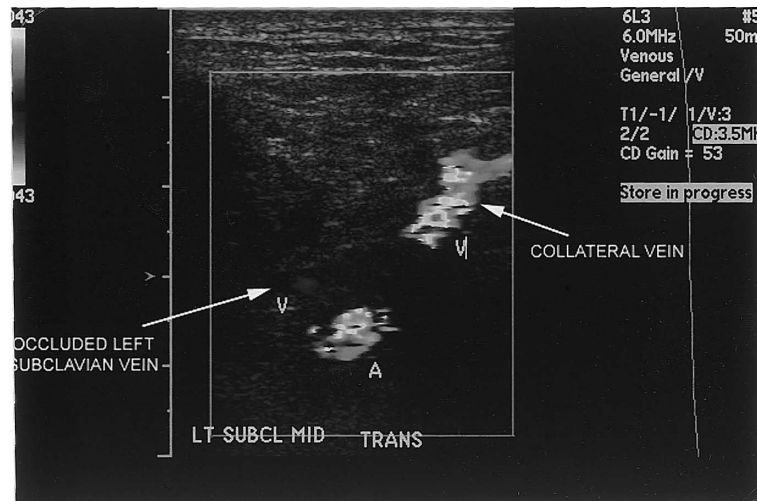


Fig. 5 Follow up transverse Doppler ultrasound image through the mid-subclavian vein shows minimal flow consistent with high grade occlusion of the vessel. Normal flow (red color) is seen in the adjacent subclavian artery. Incidentally, the color flow is seen in a nearby collateral vein, which has presumably formed in relation to the chronic DVT.

neck were ordered to evaluate the submandibular mass and rule thoracic outlet compression of the subclavian and brachial veins and brachial plexus leading to the left upper extremity swelling and weakness. The studies were unremarkable except for new lymphadenopathy in the left axilla and left subpectoral regions. The brachial plexus showed a bright signal but did not appear infiltrated as no discrete masses were identified. The patient was diagnosed with an aseptic extensive upper extremity DVT and was appropriately treated with 80 mg of Lovenox subcutaneously along with Coumadin. The patient was discharged 5 days later with Coumadin 4 mg P.O. q.i.d. The following day the patient had an FDG PET/CT scan for restaging purposes. The patient had a follow up visit 20 days after discharge at which time resolution of the left arm swelling and weakness was reported. A follow up ultrasound 3 months later showed multiple collateral vessels with chronic thrombus involving the mid left subclavian vein (Fig. 5).

PET/CT METHODS

The FDG PET/CT scan was acquired at Stanford Hospital using a Discovery LS, GE Medical Systems, Milwaukee, Wis. The PET camera of this combined scanner has a 14.6 cm axial field of view (FOV) and a transaxial resolution of 4.8 mm full-width at half-maximum at the center.

On the day of the FDG PET/CT scan, the patient had a blood sugar level of 88 mg/dl after fasting for 6 hours. 15.9 mCi (588 MBq) of F-18-FDG was then intravenously administered in the right antecubital region since the left arm was painful and swollen. Sixty minutes following the uneventful administration of the tracer, a transmission scan (5 mm contiguous axial cuts) was obtained in four integrated multi-slice helical non contrast CT, from top of the head to mid thighs. The acquisition was obtained in 2D mode at 2 minutes per bed position with a one-slice overlap at the borders of the field of view to avoid artifacts, using 140 kV, 40 mAs, and a 512 × 512 matrix size, acquiring a field of view (FOV) of 867 mm in 22.5 s. This

transmission scan was used for attenuation correction purposes and to help in anatomic localization of FDG.

Immediately afterwards, an emission scan (PET scan) was acquired in 2D mode over the same anatomical regions starting at the level of the thighs for molecular/metabolic information. The acquisition time was 5 min per bed (35 slices/bed) in 6 beds, with a one-slice overlap at the borders of the FOV. The PET emission scan was corrected using segmented attenuation data of the conventional transmission scan. A Gaussian filtering (8 mm) was performed for smoothing of images. The PET images were reconstructed with a standard iterative algorithm (OSEM, two iterative steps, 28 subsets) using GE software release 5.0.

CT data were reduced to an image matrix of 128×128 to adapt them to the PET emission scans. The images were "hardware" co-registered. The voxel size of the final coregistered PET/CT image was $3.91 \times 3.91 \times 4.25$ mm. All images were reformatted into axial, coronal, and sagittal views. They were reviewed as a rotating 3D image and in the three different axes with the software provided by the manufacturer (eNtegra, GE Medical Systems, Haifa, Israel).

RESULTS

The PET/CT study (Fig. 2) showed an intensely hypermetabolic 5×3 cm soft tissue mass in the left submandibular region, presenting an SUVmax of 22, consistent with the patient's biopsy-proven recurrent squamous cell carcinoma. An additional focus of increased FDG uptake was observed in the left cervical region at the base of the neck, corresponding anatomically with the intraluminal space of the left internal jugular vein, and presenting an SUVmax of 4.8 (Fig. 3). This finding was consistent with the known aseptic non-occlusive thrombus seen on recent ultrasound. The PET/CT study revealed also a peculiar asymmetric, moderately intense linear FDG uptake distribution in the left upper thoracic region with extension towards the medial aspect of the left arm and forearm (Figs. 3 and 4). This linear uptake seemed to follow the trajectory of the left subclavian vein, left axillary, and basilic vein to the level of the antecubital region. The maximum SUV in this territory was calculated at 2.95. These findings were interpreted as inflammatory changes along the venous system corresponding to the known left upper extremity aseptic DVT. Moderately hypermetabolic lymphadenopathy (SUVmax 3.1) was seen in the left axillary region, corresponding to up to 1.4 cm axillary lymph nodes, interpreted as reactive lymphadenopathy.

DISCUSSION

To our knowledge, only one prospective study to date has addressed the utility of FDG PET in the diagnosis of deep venous thrombosis (DVT) and deep septic thrombophle-

bitis (STP). Though costly and non-specific, FDG PET, as a functional imaging modality, offers not only obvious advantages including lack of operator dependence, whole body scanning, less dependence on body contour, anatomical position or casts and immobilization devices and being more indicative of a metabolic state, but also promising superior, clinical management discrimination between aseptic DVT and infected thrombophlebitis than purely structural studies including venography and/or ultrasound. In their limited but promising series, Miceli et al. report the superiority of FDG PET in the discrimination of STP over Doppler scan and venography in the central veins of the upper extremity, with sensitivity values of 5/5, 0/5, and 3/5, respectively.¹ Though significant FDG uptake occurred exclusively in septic thrombophlebitis (9/9) (with SUV values ranging from 3.8 to 21.4) but not in aseptic DVT (27/27) in their trials, increased FDG uptake secondary to aseptic DVT in the lower extremity has been reported,¹ a finding consistent with the acute inflammatory phase of aseptic DVT, whose existence is supported by evidence of significant polymorphonuclear aggregation and acute peaks in inflammatory markers including IL-6, IL-8, and CRP.^{2,3} The macrophages are thought to be key initiators that contribute tissue factor (TF)-bearing microvesicles that further catalyze the hypermetabolic cascade. FDG uptake by activated macrophages in infectious/inflammatory conditions has been well documented in the literature.⁴ These findings suggest that perhaps DVTs and STPs can be functionally characterized along an inflammatory spectrum. The degree of inflammation in aseptic DVT may not always exceed the threshold for PET detection, reflecting the relative hypometabolic state of aseptic DVT compared to STP. SUV kinetics analysis in STP may even play a potential role in the determination of thrombus age.

We report to our knowledge the first finding of increased FDG uptake secondary to extensive aseptic DVT in the upper extremity with PET/CT. The moderate linear FDG pattern of uptake, clearly following the trajectory of the vessels from the junction of the internal jugular and brachiocephalic vein extending distally through the subclavian and axillary to the brachial vein, presented a maximum SUV of 2.95. Though further studies are required to definitively evaluate the possible value of FDG in discriminating between aseptic DVT versus infected STP—perhaps incorporating into the definition of septic thrombophlebitis a qualitative and quantitative molecular imaging description encompassing standard uptake value (SUV) distribution and threshold analysis—we concur with Miceli's study that the non-invasive FDG PET/CT may become a sensitive and specific test for the spatial and temporal evaluation of septic thrombotic events of the deep venous system of areas anatomically less accessible by non-invasive conventional means. PET studies have played a crucial role in the diagnostic work-up and subsequent management of fever of unknown

origins at the portal vein and aorta.⁵⁻⁸ Because upper extremity DVT is frequently clinically asymptomatic or atypical, especially in immunocompromised, leukopenic chemotherapy patients, and children, and because axillary-subclavian venous thrombosis (ASVT) develops in up to 28% of chronic indwelling catheter patients,⁹ it may be reasonable to flag cancer patients with central venous catheters undergoing routine FDG PET/CT staging/re-staging for screening of upper extremity thrombosis as this would not incur additional costs. Regardless of FDG-PET's role in thrombus characterization, nuclear medicine physicians should become familiar with this pattern of FDG uptake, especially in reading PET and PET/CTs in patients with known carcinoma or chronic indwelling catheters.

REFERENCES

1. Miceli M, Atoui R, Walker R, Mahfouz T, Mirza N, Diaz J, et al. Diagnosis of Deep Septic Thrombophlebitis in Cancer Patients by Fluorine-18 Fluorodeoxyglucose Positron Emission Tomography Scanning: A Preliminary Report. *J Clin Oncol* 2004; 22 (10): 1949-1956.
2. Roumen-Klappe EM, den Heijer M, van Uum SH, van der Ven-Jongekrijg J, van der Graaf F, Wollersheim H. Inflammatory response in the acute phase of deep vein thrombosis. *J Vasc Surg* 2002; 35 (4): 701-706.
3. Stewart GJ. Neutrophils and deep venous thrombosis. *Haemostasis* 1993; 23 Suppl 1: 127-140.
4. Viles-Gonzalez JF, Fuster V, Badimon JJ. Thrombin/inflammation paradigms: a closer look at arterial and venous thrombosis. *Am Heart J* 2005; 149 (1 Suppl): S19-31.
5. Bleeker-Rovers CP, Jager G, Tack CJ, Van Der Meer JW, Oyen WJ. F-18-fluorodeoxyglucose positron emission tomography leading to a diagnosis of septic thrombophlebitis of the portal vein: description of a case history and review of the literature. *J Intern Med* 2004; 255 (3): 419-423.
6. Raman S, Nunez R, Oliver Wong C, Dworkin HJ. F-18 FDG positron emission tomographic image of an aortic aneurysmal thrombus. *Clin Nucl Med* 2002; 27 (3): 213-214.
7. Jensen RB, Mortensen J, Dreyer M. Acute deep venous thrombosis and PET scanning with 2-fluoro-2-deoxy-D-glucose, FDG. *Ugeskr Laeger* 2001; 163 (38): 5209-5211.
8. Kikuchi M, Yamamoto E, Shiomi Y, et al. Case report: internal and external jugular vein thrombosis with marked accumulation of FDG. *Br J Radiol* 2004; 77: 888-890.
9. Verso M, Agnelli G. Venous thromboembolism associated with long-term use of central venous catheters in cancer patients. *J Clin Oncol* 2003; 21 (19): 3665-3675.